Composites Science and Technology 248 (2024) 110461

Contents lists available at ScienceDirect

Composites Science and Technology

journal homepage: www.elsevier.com/locate/compscitech

Modeling approaches for ballistic simulations of composite materials: Analytical model vs. finite element method

Dayou Ma *, Riccardo Scazzosi, Andrea Manes

Politecnico di Milano, Department of Mechanical Engineering, via la Masa, 1, 20156, Milan, Italy

ARTICLE INFO

Keywords:
Full metal jacket projectile
Kevlar/epoxy composite
Ghost projectile method
0.357 magnum
MAT_162

ABSTRACT

Development of predictive models for woven composite materials under ballistic impact is of great importance for their further applications as protective structures in aerospace and related fields. There are mainly two numerical methodologies widely used in the community: analytical models and finite element methods. As a popular method, finite element modeling has been widely investigated and applied in ballistic simulations, which can provide accurate results. However, high time consumption and complex calculation process cannot be avoided due to the complicated fiber architecture of woven composites. Alternatively analytical modelling approaches can provide a reliable prediction for ballistic simulation through a relatively portable modeling process with a high computational efficiency. However, limited attention has been paid to replicating the ballistic behavior of deformed projectiles versus woven composites, especially with a full metal jacket projectile. Therefore, in the current work the capability of different numerical modeling methods to simulate ballistic behaviors of woven composites impacted by a full metal jacket projectile is investigated. For analytical models, an innovative approach named ghost projectile method has been proposed with the focus on the effect of the deformable jacket of the projectile during impact loading. Regarding the finite element method, damage assessment by MAT_162 in Ls-dyna was used with optimized parameters. Experimental data on a Kevlar tile impacted by a full metal jacket projectile (0.357 Magnum) was used as a reference for comparison with numerical models. The capability of the two different numerical modeling methodologies in the current work was compared with respects to the ballistic curves, load history and projectile deformation.

1. Introduction

With the high demand of light weight materials, more and more composites have been applied in aerospace and related fields. Woven composites have been paid great attention for the potential applications as protective structures, due to excellent mechanical properties exploited during ballistic impact. Several experimental activities on ballistic tests have been conducted to reveal the mechanical responses of woven composites under ballistic impact. As reported in Cavallaro's work [1], the fiber architecture has significant effect on the impact resistance of composites. Complex fiber architecture inside woven composites provides high impact resistance under ballistic loading but also challenges the predictions on their mechanical properties and damage behaviors which involves different damage mechanisms like fiber bending and delamination [2,3]. On the other hand, damage detection of woven composites requires specific technologies, such as X-ray [4] and Ultrasonic imaging [5], and/or sample cutting for cross-sectional inspection [6] to characterize different failure mechanisms. Considering experimental costs and safety issues during the ballistic impact, the development of numerical methods is helpful to improve investigation about woven composites.

The most popular numerical methods widely applied in the community to replicate the mechanical response under ballistic impact are the finite element method and analytical modeling. For woven composites, the application of finite element method allows the introduction of full detailed fiber architecture at different scales [6,7], the results of which advances the ballistic simulation [8,9]. Apart from the reconstruction of geometry, another key point for the modeling of woven composites is the determination of damage assessment models [10,11], which enables to distinguish different failure modes [8,12], and provides a smooth failure envelope [13,14]. Among these damage models, an excellent performance of MAT_162 in Ls-dyna, has been reported in terms of high predictive accuracy [15,16]. However, the determination of parameters in MAT_162 is complicated due to the large number of

* Corresponding author.
E-mail address: dayou.ma@polimi.it (D. Ma).

https://doi.org/10.1016/j.compscitech.2024.110461
Received 13 November 2023; Received in revised form 18 January 2024; Accepted 19 January 2024
Available online 27 January 2024

input parameters that have relevant effects on the modeling results for composites under impact loading condition [17–19].

Compared to the finite element method, the use of analytical modeling approaches for ballistic simulation requires less efforts of model generation and calculational costs. However, analytical modeling approaches potentially lack generality (generally they are fitted to specific and simple cases) and need careful selection of the appropriate physics to be reproduced. The deformation of composites [20], as well as damage evolution in the manner of delamination [21], matrix cracking [22] and fiber breakage [23], even the interaction among them [24], can be replicated by means of analytical models with limited calculation costs [25,26]. The deformation of the impacted target was modelled in a cone or V-tent shape, which can be formulated according to the spread of stress waves, thus resulting in the deformation during impact loading [6]. Considering the modeling of damage, generally energy-based methods are applied to calculate energy dissipated by damage accumulation of different mechanisms, which can be later combined with the deformation of the impactor to obtain the overall energy dissipation [26,27]. For woven composites, the primary and secondary yarns can be defined according to whether the projectile directly contacts related regions at each time step, which can better model the mechanical degradation of impacted panels due to the deformation/energy absorption as the strain wave propagates [6,27]. However, several parameters are involved in an analytical model for an accurate replication of the ballistic behavior of woven composites and some assumptions are introduced to simplify the analytical modelling; generally, most of the simplifications regard the projectile as the primary focus is usually put on the modeling of targets. The projectile was mostly modelled as a rigid body [28], or a partially rigid body [27]. In reality, a soft-core projectile is often used which provides different damage behaviors compared with cases of rigid projectiles. A full metal jacket projectile (FMJ) [8,29], is one of the typical bullets, which includes two materials: one acts as the jacket, and the other is used as the core, presenting various mechanical behaviors during the impact process. In order to simulate the loss of projectile's mass during impact, a fragment-based projectile method was proposed to account for the failure of the projectile [26]. In Ref. [30] the equivalent projectile method was created to combine the mechanical properties of the jacket and core for the replication of the projectile's deformation during the impact. However, neither of these methods can consider the different behaviors of the jacket and core of projectiles. As indicated according to the deformation filmed in experiments [29] and numerical results from finite element methods [8], the jacket presents high stiffness for small deformation at the beginning of loading, and the core starts to be exposed to quick and large deformation after the failure of the jacket. As a result, an accurate modeling of both components of the FMJ projectile is of great importance for the modeling of ballistic tests. While analytical modeling requires some extra efforts, the separate modeling of each component of the projectile is directly achievable by finite element methods.

In the present work, a ghost projectile method was proposed, based on a comprehensive review [30–32] of the analytical modeling on the ballistic behavior of woven composite, which can improve the existing models and consider the separate mechanical mechanisms for the jacket and core of FMJ projectiles during the impact loading. Besides, a finite element model was also built in the current work with optimized MAT_162 in Ls-dyna as a damage assessment model of woven composites. In order to validate both modelling approaches, ballistic tests on plain woven composites of Kevlar fiber with 0.357 magnum projectile were carried out. The experimental and numerical results were compared and analyzed with respects to the ballistic curve, the loading history and the deformation of the projectile, and capability of analytical model and finite element method investigated.

2. Numerical methodologies

2.1. Analytical model

2.1.1. Analytical model on woven composites

An energy-based method is regarded as an efficient way for the simulation of the ballistic behavior of woven composites. In an energy-based analytical model, the formulation of the ballistic behavior was established through the balance of the total energy ($E_{k,tot}$), which can be contributed to the kinetic energy of the deformed tip of the composite target ($E_{k,t}$), energy absorbed by the deformation of target (E_{def}), energy absorbed by shear plugging of the composite (E_{sp}), energy dissipated by delamination and matrix cracking (E_{del} & E_{mc}), as well as the remaining kinetic energy of the projectile ($E_{k,p}$) [31], as listed in Equation (1), where i represents ith time step.

$$E_{k,tot,i} = E_{k,t,i} + E_{def,i} + E_{sp,i} + E_{del,i} + E_{mc,i} + E_{k,p,i} \tag{1}$$

As the projectile is rigid during the impact, the velocity of the target tip can be treated as the same as the projectile considering their direct contact, which can determine the kinetic energy of the deformed tip of the composite target ($E_{k,t}$).

Regarding the deformation of the target, the first concern is the deformed area, which can be defined by the wave theory according to the analysis based on the experimental observation [33,34]. The propagated velocity, c, of the stress wave inside the material can be defined by the material's modulus (E) and density (ρ) based on Equation (2). In the case of ballistic impact, the input loading starts from one contact point in the target, thus the stress wave can be propagated in both longitudinal and transverse directions. The longitudinal stress wave speed can be determined by Equation (2), while the transverse one can be calculated based on the stress and strain field according to Equation (3). The travel of the stress wave can be used to determine the deformed area based on Equation for the radii of the composite conoid deformation (r_{con}) and longitudinal wave covered area (r_l) in each time interval Δt during the calculation as presented in Equation (4). As the area of the deformed conoid area can be calculated, the mass of deformed conoid can be obtained with deformed area and the thickness (h) of the target based on Equation (5), which can be used for its kinetic energy.

$$c_L = \sqrt{E/\rho} \tag{2}$$

$$c_T = \sqrt{(1+\varepsilon)\sigma/\rho} - \int_0^{\varepsilon} \sqrt{d\varepsilon/\rho d\sigma} d\varepsilon \tag{3}$$

$$\begin{aligned} r_{con,i} &= \sum_{i=0}^{i} c_T \bullet \Delta t \\ r_{l,i} &= \sum_{i=0}^{i} c_L \bullet \Delta t \end{aligned} \tag{4}$$

$$m_{con,i} = \pi r_{con,i}^2 h\rho \tag{5}$$

$$\varepsilon(x)_i = \left(\frac{\sqrt{r_{con,i}^2 + z_i^2} - r_{con,i}}{b^{L/a} - 1} \right) \frac{ln(b)}{a} \bullet b^{x/a} \tag{6}$$

For woven composites, the yarns are surrounded by matrix, and this provokes a different mechanical response under impact loading compared to homogenous materials. As a result, accurate modeling of the location of the yarns can improve the accuracy of the analytical model, leading to the different formulation on primary and secondary yarns, while the mechanical response of the matrix was regarded, focusing on the yarns, till its cracking. Besides, considering the fiber architecture of the woven composites is quite complex, interlacing both warp and weft yarns, introducing primary and secondary yarns into calculation can simplify the modeling process. As mentioned in Section

1, the primary yarns are the ones in direct contact with the projectile, while it is the opposite for the secondary ones, as visible in Fig. 1. For primary yarns, the deformation can be modelled according to the distribution of strain in the conoid deformed region of the target considering the distance from the impact center, x, as listed in Equation (6). Here, L is the total length of the yarns; a is the width of yarn; b is a constant to represent the transmission factor of the stress wave in the related materials, which is only related to the geometry of woven model in this case. Besides, z here is the depth of the conoid region of the target, which is equal to the distance travelled by projectile.

Considering the secondary yarns, the equation for the deformation is similar as the primary yarns, but the degradation of the input impulse due to the impact is considered. Thus, r_{con} should be replaced by $r_{sec,i} = \sqrt{r_{con,i}^2 - x^2}$, leading to the strain on the secondary yarns which can be described as Equation (7)

$$\dot{\varepsilon}(x)_i = \left(\frac{\sqrt{r_{sec,i}^2 + z_i^2} - r_{sec,i}}{b^{L/a} - 1}\right) \frac{ln(b)}{a} \bullet b^{x/a} \tag{7}$$

Shear plugging is always regarded as one of the main failure mechanisms during the impact of composite materials [6]. The shear stress (τ) near the impact point on the target can be obtained through Equation (8), where F is the force exerted by projectile, calculated by mass of projectile multiplying the acceleration in each time step, R_p is the radius of the projectile, and h_{sp} is the thickness of composite involved in failure due to shear plugging. The failure thickness due to shear plugging can be defined when the shear stress meets the shear plugging strength (τ_{sp}). The shear plugging occurs as the threshold strength (S_{sp}) is met, which can determine h_{sp}. The absorbed energy by shear plugging can then be expressed as Equation (9).

$$\tau = \frac{F}{2\pi R_p h_{sp}} \tag{8}$$

$$E_{sp} = 2\pi R_p S_{sp} h_{sp}^2 \tag{9}$$

Considering the similar mechanism for the interface between layers and the matrix cracking, E_{del} and E_{mc} are discussed here together. Generally, a time-based equation was used to describe the absorbed energy due to these damage mechanisms [6,31] considering the propagation of the delaminated area in each time interval defined by its radius, r_d, as expressed below:

$$\Delta E_{del,i} = \pi K_{del}\left(r_{d,i+1}^2 - r_{d,i}^2\right) G_{II} \tag{10}$$

$$\Delta E_{mc,i} = \pi K_{mc}\left(r_{d,i+1}^2 - r_{d,i}^2\right) E_m h V_m \tag{11}$$

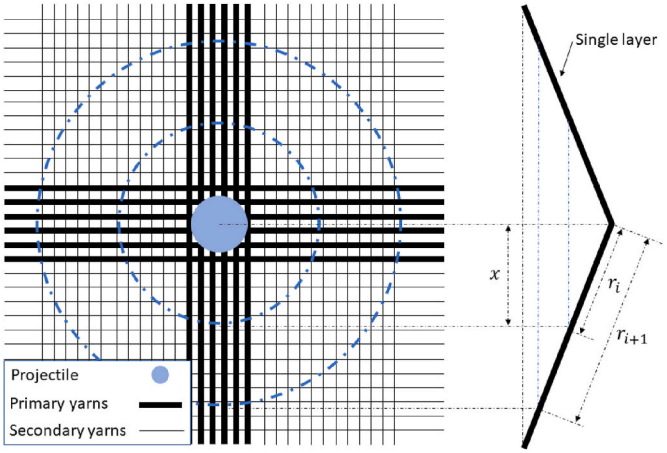

Fig. 1. Schematic for different yarns in analytical model.

where G_{II} is the critical energy release rate for the delamination (model-II fracture, as the typical failure mode of delamination), E_m is the threshold energy for the matrix cracking, V_m is the volume fraction of the matrix in composite, and h is the thickness of the target. Besides, K in equations is the parameter for the calibration of the delamination and matrix cracking.

As summarized here, the formulation of Equation (1) with respects to different energy dissipated can be regarded as the base layer of the analytical model for the ballistic behavior of woven composites in the present work, which has been validated by experimental data related to different composite materials [25,31]. Based on the understanding of the mechanical and damage behaviors of woven composites under ballistic impact, the analytical model has been adapted with more dissipated energy decompositions considered on the right side of Equation (1) [32].

In order to achieve a precise description of the deformation of composites in each layer, the first one added was the energy absorbed by the target under compression [32]. As the projectile starts touching the target, the compression along the thickness occurs in the region affected by the impact impulse, which can transfer part of the kinetic energy towards compressive deformation of the target. For the region in direct contact, the compressive strain is constant, while a linear degradation of the strain can be applied to describe the remaining region in compression, leading to Equation (12). Compared with the original equation on compressive strain, a geometry factor, α, was introduced here considering the variation on the contact area due to the different shapes of the projectile, which can be determined by the obliquity of the tip on the projectile [35]. The energy dissipated by the compressive deformation of the composite can be obtained according to Equation (13) knowing the modulus of the target.

$$\varepsilon_{com,i}(x) = \begin{cases} \dfrac{z_i}{h}, x \le \alpha R_p \\ \dfrac{z_i x}{h r_{con,i}}, x > \alpha R_p \end{cases} \tag{12}$$

$$E_{com,i} = \pi\alpha^2 R_p^2 h \int_0^{\alpha R_p} E(x)\varepsilon_{com,i}(x)dx + 2\pi h \int_0^{r_{con,i}} \int_{\alpha R_p}^{r_{con,i}} E(x)\varepsilon_{com,i}(x) r dr dx \tag{13}$$

Besides, the significant contribution of bending deformation from the impact simulation of composite materials has been reported with numerical method [36]. Energy dissipated by bending deformation can improve the accuracy of the analytical model on the ballistic prediction [32]. The bending deformation can be calculated according to Equation (14) based on thin plate theory in the plane-stress state, where the bending deformation can be regarded as a chord system [32]. Here, M is the bending moment for the bending region of target and ν is the Poisson ratio of the target.

$$\begin{cases} M_i = \dfrac{4\pi(2+\nu)D}{r_{con,i}} z_i \\ E_{bending,i} = M_i \dfrac{2z_i}{r_{con,i}} \end{cases} \tag{14}$$

As a result, the energy absorbed by the deformation of the target can be regarded as a summary of energy due to deformation of primary yarns ($E_{def,pri}$), deformation of secondary yarns ($E_{def,sec}$), deformation of conoid area (E_{con}), bending deformation ($E_{bending}$) and compressive deformation (E_{com}), as presented in Equation (15). Accurate results can be provided after the optimization of energy absorbed by deformation considered in Equation (1).

$$E_{def,i} = E_{def,pri,i} + E_{def,sec,i} + E_{con,i} + E_{bending,i} + E_{com,i} \tag{15}$$

2.1.2. Analytical model on projectile

Based on the assumption of the rigid projectile, the role of the pro-

jectile in the analytical model is to provide the initial total kinetic energy, causing the deformed shape of the target at its tip, and eventually detaching the target with the remaining kinetic energy at the end of the calculation, or set as a flag for the termination of the analytical model in case of zero remaining kinetic energy. The (remaining) kinetic energy can be easily calculated based on Equation (16), where v_i is the velocity of the projectile, and m_p is the mass of the projectile, which is a constant for a rigid body.

$$E_{k,p,i} = \frac{1}{2} m_p v_i^2 \tag{16}$$

However, modeling a soft core projectile in a rigid fashion can hardly replicate the behavior of the impact with woven composites, which leads to the importance of the consideration of an analytical model with a deformed projectile [37]. Compared to the rigid body method, an updated area of cross-section (A_p) and length (L_p) of the projectile must be considered in the analytical model as listed with Equation (17)(18). Here ρ_p and Y_p are the density and the yield strength of the projectile, while $K_{\Im}$ is named as impedance matching factor, used to describe the motion of the interface between the projectile and target [35]. K_{im} can be determined with the density and stress wave speed of both the projectile (ρ_p, C_p) and target (ρ, C_t) based on Equation (19). The value of K_{im} can represent the softness of the projectile compared to the target: a larger K_{im} indicates a softer projectile compared to the same target, while $K_{im} = 1$ means the rigid projectile. Moreover, for the overall analytical model, attention should be paid on the previous equations related to the length and/or area of the projectile, which should be adapted with various values in each time step for a deformed projectile.

$$L_{p,i+1} = L_{p,i}\, exp\left\{\frac{-\rho_p}{2Y_p}\left[\left(\frac{v_i}{K_{im}}\right)^2 - \left(\frac{v_{i+1}}{K_{im}}\right)^2\right]\right\} \tag{17}$$

$$\frac{\left(A_{p,i+1} - A_{p,i}\right)^2}{A_{p,i+1}A_{p,i}} = \frac{3\rho_p v_i^2}{2K_{im}Y_p} \tag{18}$$

$$K_{im} = 1 + \rho_p C_p \Big/ \left[\rho_t \sqrt{K_t/\rho_t}\right] \tag{19}$$

The application of FMJ projectile introduces complexity to the development of analytical model. A previous work [30] about analytical modeling of a deformed projectile exploits a homogeneous equivalent projectile. Two different materials on FMJ for jacket and core cannot be described through Equations 17–19. As a results, the equivalent projectile method proposed for FMJ [30], uses adapted material parameters in Equations 17–19 to combine both the jacket and core in order to use homogenous material parameters. The adapted parameters are calculated to keep the density and the plastic wave speed the same as the FMJ projectile and to guarantee the total mass of the projectile. Nevertheless, due to the significant difference between the mechanical responses of the jacket and core of the projectile, the equivalent projectile method provides only limited improvement of the analytical model.

In the current work, a ghost projectile method was proposed to replace the equivalent projectile method, which can separately consider the core and jacket of the projectile. The basic concept of the ghost projectile method is presented in Fig. 2. The equivalent projectile introduced before is used as a ghost projectile in this analytical model, which can provide the guideline for the deformation and erosion of the projectile (D_p). The deformation obtained from the ghost projectile is compared to the thickness of the jacket (t_j). According to the state of the projectile, the algorithm on the deformation of projectile, i.e. Equations 17–19, can be updated: Y_p, ρ_p and C_p are used, as the material of the jacket, when the erosion of the projectile is smaller than the thickness of the jacket ($D_p < t_j$); while the values of Y_p, ρ_p and C_p , the material of core, if the erosion of the projectile is greater than the thickness of the jacket ($D_p \geq t_j$). Through this method, the jacket and core of the projectile can be considered separately. It is noted that the friction between the composite and projectile was not considered because the dissipation of energy due to friction can be negligible compared to the one absorbed by deformation of the projectile.

All the parameters introduced before, regarded as input parameters applied in the analytical model, are present in Table 1 in the current case. More details about the materials can be found in Section 3.

2.2. Finite element method

2.2.1. Numerical modeling

A numerical model is another popular method for the ballistic simulation, especially for complex structures. For instance, separately modeling the jacket and core of projectile in the finite element method can be achieved as presented in Fig. 3a. For the composite target, a

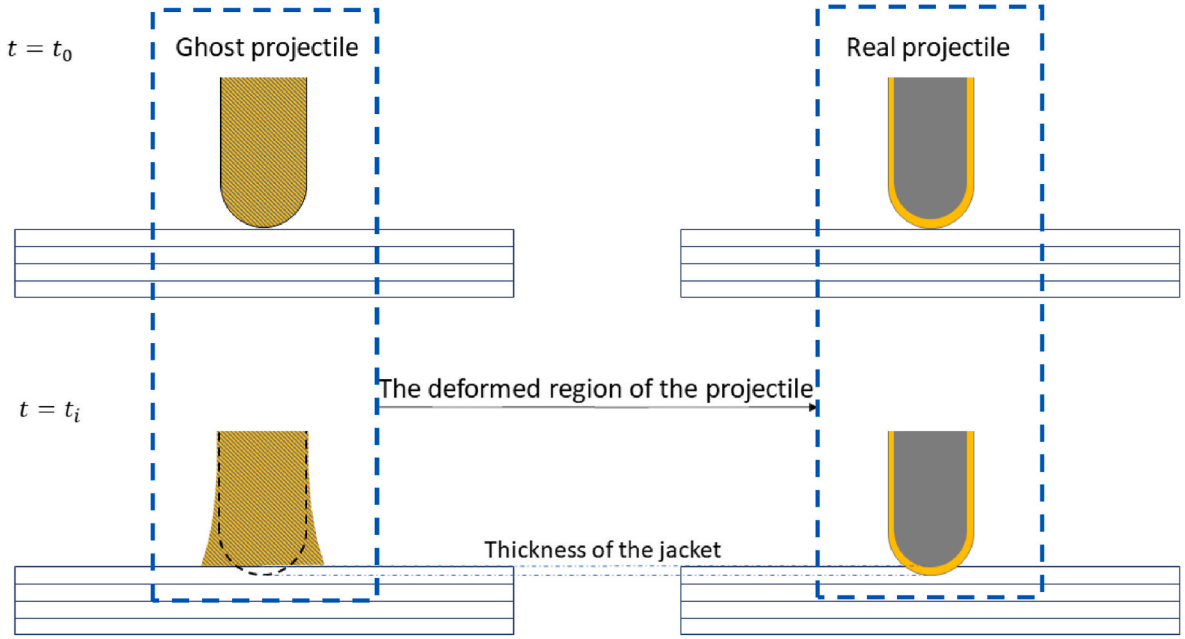

Fig. 2. Schematic for ghost projectile method.

Table 1
Input parameters for the target and projectile in the analytical model.

Material	Properties	Parameters	Notes
Composite target			
Kevlar 29/ Epoxy	ρ, $kg \bullet m^{-3}$	1025	Density of the target
	h, mm	6.7	Thickness of the target
	N	14	Number of layers
	V_f	0.63	Volume fraction of fiber
	E, GPa	80	Elastic modulus of fiber
	E_{th}, GPa	6	Out-of-plane modulus
	b	0.9	transmission factor
	G_{II}, $J \bullet m^{-2}$	1000	Critical energy release rate for delamination
	E_m, $kJ \bullet m^{-3}$	900	Threshold energy for the matrix cracking
	b, mm	0.25	Thickness of the fiber
	K_{del}	1	Calibrated parameter for delamination
	K_{mc}	1	Calibrated parameter for matrix cracking
Projectile			
Ghost projectile	$\rho_{p.eq}$, $kg \bullet m^{-3}$	10409	Equivalent density of the projectile
	$Y_{p.eq}$, MPa	106.5	Equivalent yield strength of the projectile
Jacket of projectile	$\rho_{p.j}$, $kg \bullet m^{-3}$	8250	Density of the brass for jacket
	$Y_{p.j}$, MPa	344.7	Yield strength of the brass for jacket
Core of projectile	$\rho_{p.c}$, $kg \bullet m^{-3}$	10660	Density of the lead for core
	$Y_{p.c}$, MPa	56.5	Yield strength of the lead for core

homogeneous model was built according to the geometry of the target as shown in Fig. 3b. In each layer, one element is built along the thickness, while the size of the mesh was 1.0 mm as validated in Ref. [16]. Considering the boundary conditions of the finite element method, a symmetric boundary was used for a quarter model to reduce the calculation cost as visible in Fig. 3c, while the fixed boundary condition was applied on the other edges to replicate the clamping of the fixture in ballistic tests as mentioned in Ref. [38]. Regarding the contact behavior between the projectile and the target, the eroding contact (ERODING_SURFACE_TO_SURFAC) was applied [39].

2.2.2. Damage assessment models

A transverse isotropic homogeneous material model was used to describe the elastic mechanical behaviors of woven composites in the current case. Considering the homogeneous approach to the modeling of the woven composites, the damage assessment is of great importance. Plenty of works have been carried out to evaluate the capability of different damage models during impact loading [10,19,36]. Among them, MAT_162 in Ls-Dyna provides accurate predictions [19], leading to its wide application [18,40]. In MAT_162, the tensile-shear failure mode of the fiber is defined by Equation (20), where E_a is the elastic modulus along a direction (one of the in-plane direction), G_{ca} is shear modulus, and S_{aT} and S_{aFS} are the tensile and shear strength in the related directions. Herein, the two in-plane directions share the same mechanical behavior, indicating that the equations on failure modes are the same for the a and b direction.

$$f_{st} = \left(\frac{E_a \varepsilon_1}{S_{aT}}\right)^2 + \left(\frac{G_{ca} \varepsilon_{13}}{S_{aFS}}\right)^2 \tag{20}$$

The compressive failure mode of the fiber is expressed by the compressive strength of fiber (S_{aC}) according to Equation (21). On the other hand, the crush failure of the fiber can be determined by Equation (22), where S_{FC} is the strength of the crush failure.

$$f_c = \left[\frac{E_a\left(\varepsilon_1 + \langle \varepsilon_3 \rangle \frac{E_a}{E_c}\right)}{S_{aC}}\right]^2 \tag{21}$$

$$f_{fc} = \left(\frac{E_c \varepsilon_3}{S_{FC}}\right)^2 \tag{22}$$

As for the matrix failure, the in-plane failure and delamination have been considered in the model based on Equation (23)&(24), where S_{ab} is the in-plane shear strength, S_{cT} is the tensile strength along the thickness, and S_{bc} and S_{ac} are the out-of-plane shear strength for composites. Besides, a scale factor S is introduced to calibrate the numerical model with experimental data involved. For an accurate modeling of the matrix failure, the Coulomb's friction angle (Φ) is considered in cracking strength of S_{SRC}, which is determined by $S_{SRC} = E_c \tan \Phi \varepsilon_3$.

$$f_m = \left(\frac{G_{ab} \varepsilon_{12}}{S_{ab}}\right)^2 \tag{23}$$

$$f_{del} = S^2\left[\left(\frac{G_c \varepsilon_3}{S_{cT}}\right)^2 + \left(\frac{G_{bc} \varepsilon_{23}}{S_{bc} + S_{SRC}}\right)^2 + \left(\frac{G_{ac} \varepsilon_{13}}{S_{ac} + S_{SRC}}\right)^2\right] \tag{24}$$

In order to precisely model the damage behaviors, the strain rate effect is considered (see Equation (25)), which has a significant influence on the ballistic simulation of woven composites [8,41]. Here $\{X_{rate}\}$ is the related mechanical parameters, i.e., modulus and strength, at a strain rate of $\dot{\varepsilon}$, and $\{X_0\}$ is the initial values at the referenced strain rate ($\dot{\varepsilon}_0$).

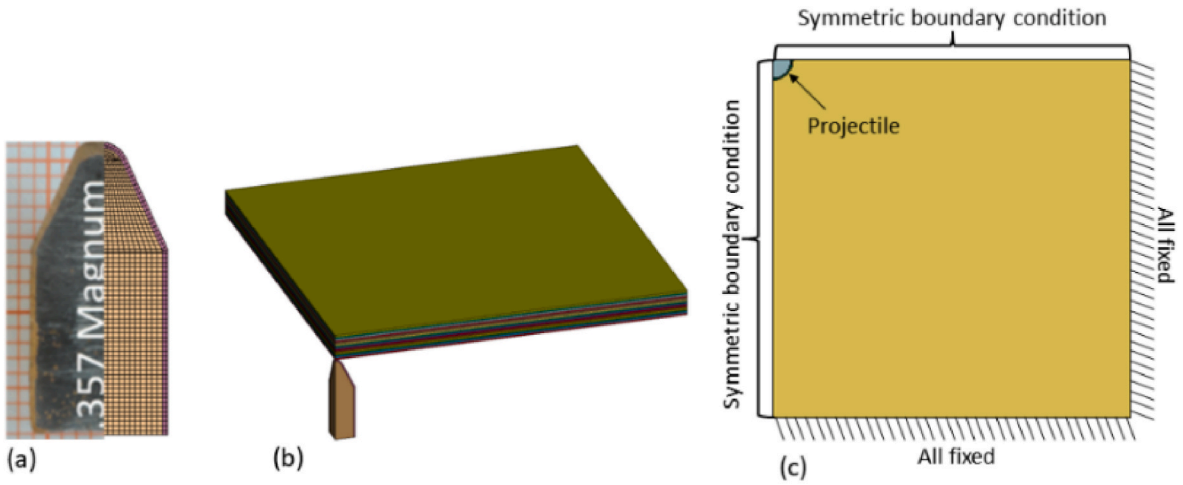

Fig. 3. Finite element modeling on projectile (a) and woven composite (b) with their boundary conditions (c).

$$\{X_{rate}\} = \{X_0\}\left[1 + C_{rate}\, ln\left(\frac{\dot{\varepsilon}}{\dot{\varepsilon}_0}\right)\right] \tag{25}$$

However, MAT_162 has several parameters which need numerical calibration for a specific material before the application, as carried out by Scazzosi et al. for Kevlar/epoxy [16] concerning the element erosion and hourglass control of the finite element method.

Regarding the projectile, the Johnson-Cook model [42] with Cockcroft-Latham failure criterion [29], named MAT_107 in Ls-dyna, was used on both the jacket and core, but with different parameter inputs according to their materials. The Johnson-Cook model was described by Equation (26), where A, B, C, n, m are the parameters for the description of flow stress according to strain and strain rate hardening and T_0 and T_m are the referenced and melting temperatures. The failure of the material is determined by the Cockcroft-Latham failure criterion, the element can be removed from the model when the Cockcroft-Latham parameter W_{CR}, as defined in Equation (27), reaches a critical value.

$$\overline{\sigma} = (A + B\varepsilon^n)\left(1 + Cln\frac{\dot{\varepsilon}}{\dot{\varepsilon}_0}\right)\left[1 - \left(\frac{T - T_0}{T_m - T_0}\right)^m\right] \tag{26}$$

$$W_{CR} = \int_0^{\varepsilon_f} \overline{\sigma} d\varepsilon \tag{27}$$

The numerical inputs of the mechanical behavior of the materials involved in the finite element model are listed in Table 2, which can be also found in Refs. [16,30] with some parameters optimized for specific target (Kevlar 29) in the current work. More details on the materials involved in the current case can be found in Section 3.

3. Experimental validation

As a validation and a reference for the capability study on the finite element method and analytical model, experimental data from ballistic tests with composite materials impacted by FMJ was utilized. The composite target with a dimension of 270 × 270 × 6.5 mm^3 and a density of 1025 $kg/m^3$was manufactured with Kevlar 29 plain weave fabrics and epoxy resin named Microtex E9. 14-layer composites were used. More details of the composite materials can be found in Ref. [30]. As for the FMJ projectile, 0.375 magnum was used (see Fig. 3a), which contains brass as the jacket and lead as the core. Considering the experimental setup for the ballistic tests as presented in Fig. 4a, the gun was fixed 5 m away from the target. For each shot, the impact was targeted at the center of the composite panel and perpendicular to the target panel. The impact velocity of the projectile was set in the range from 300 m/s to 700 m/s. In order to record the impact and residual velocities of the projectile, two velocity screens were placed 2.5 m in front of the target and towards the back side of the target. Considering the window fixture as shown in Fig. 4b was used to clamp the target here, the dimension for the target in numerical models should be 160 × 160 mm^2 (80 × 80 mm^2 for quarter modeling). The parameters of the material model used for the analytical model and finite element method can be found in Table 1 and 2.

4. Results and discussions

The results from the analytical model and finite element method for the simulation of the ballistic behavior of Kevlar/epoxy composite were compared with respects to the ballistic curves, the damage phenomena as well as the load history of projectile. The experimental data were used as reference for the capability study of these numerical methods.

Considering that the analytical model was updated for the FMJ projectile, the accuracy of the ghost projectile method should be validated as the first step. The comparison on the ballistic curve of the composite target among the experimental data and different analytical models is presented in Fig. 5. The relation between the impact and residual velocities was built interpolating the results by mans of Lambert-Jonas (L-J) model [43]. The accuracy of the simulation with the rigid projectile method cannot be guaranteed because the deformation and damage of the projectile during the impact loading can lead to more energy dissipated by the projectile, resulting in different mechanisms between the rigid and deformed projectile. The error between the rigid projectile method and experimental data can be significantly reduced if the projectile is set as a deformed one, as the equivalent projectile method. But the accuracy of the analytical model can be further improved with the ghost projectile method, which can separately consider the core and jacket of the FMJ projectile.

Numerical FEM model can also be compared with the experimental data as shown in Fig. 6a. The difference on the description of the ballistic curve is located on the low velocity. However, both the analytical model and finite element method provide comparable results on the residual velocity when the impact velocity is larger than 415 m/s (as marked in the figure), after which a linear relationship between the residual and

Table 2
Input parameters for the target (MAT_162) and projectile (MAT_107) in the finite element method.

Material	Properties	Parameters	Notes
Composite target			
Kevlar 29/ Epoxy	ρ, $kg \bullet m^{-3}$	1025	Density of the target
	$E_a = E_b$, GPa	10	In-plane modulus (a, b direction)
	E_c, GPa	6	Out-of-plane modulus (c direction)
	G_{ab}, GPa	0.77	Shear modulus of ab-plane
	$G_{bc} = G_{ca}$, GPa	5.43	Shear modulus of bc, ca plane
	ν_{ab}	0.25	Poisson's ratio in ab plane
	$\nu_{bc} = \nu_{ca}$	0.33	Poisson's ratio in bc/ca plane
	$S_{aT} = S_{bT}$, MPa	405	Tensile strength along a/b direction
	$S_{aC} = S_{bC}$, MPa	185	Compressive strength along a/b direction
	S_{ab}, MPa	77	Shear strength of ab plane
	$S_{bc} = S_{ca}$, MPa	898	Shear strength of bc/ca plane
	S_{FC}, MPa	1200	Crush strength of fiber
	S_{del}	0.3	Scale factor for delamination
	Φ, °	10	Coulomb's friction angle
	AM1	0.5	Coefficient for the strain softening 1
	AM2	0.5	Coefficient for the strain softening 2
	AM3	1	Coefficient for the strain softening 3
	AM4	5	Coefficient for the strain softening 4
	C_{rate1}	0.0257	Coefficient for strain rate effect 1
	C_{rate2}	0.0246	Coefficient for strain rate effect 2
	C_{rate3}	0.0246	Coefficient for strain rate effect 3
	C_{rate4}	0	Coefficient for strain rate effect 4
Projectile			
Brass (jacket)	E, GPa	115	Elastic modulus
	ν	0.31	Poisson's ratio
	A, MPa	111.7	Johnson-Cook coefficient A
	B, MPa	504.7	Johnson-Cook coefficient B
	n	0.42	Johnson-Cook coefficient n
	C	0.0085	Johnson-Cook coefficient C
	T_m, K	1189	Melt temperature
	m	1.68	Johnson-Cook coefficient m
	W_{cr}, MPa	914	Cockcroft-Latham strength
Lead (core)	E, GPa	16	Elastic modulus
	ν	0.42	Poisson's ratio
	A, MPa	0	Johnson-Cook coefficient A
	B, MPa	55.5	Johnson-Cook coefficient B
	n	0.0987	Johnson-Cook coefficient n
	C	0.126	Johnson-Cook coefficient C
	T_m, K	525	Melt temperature
	m	1.0	Johnson-Cook coefficient m
	W_{cr}, MPa	175	Cockcroft-Latham strength

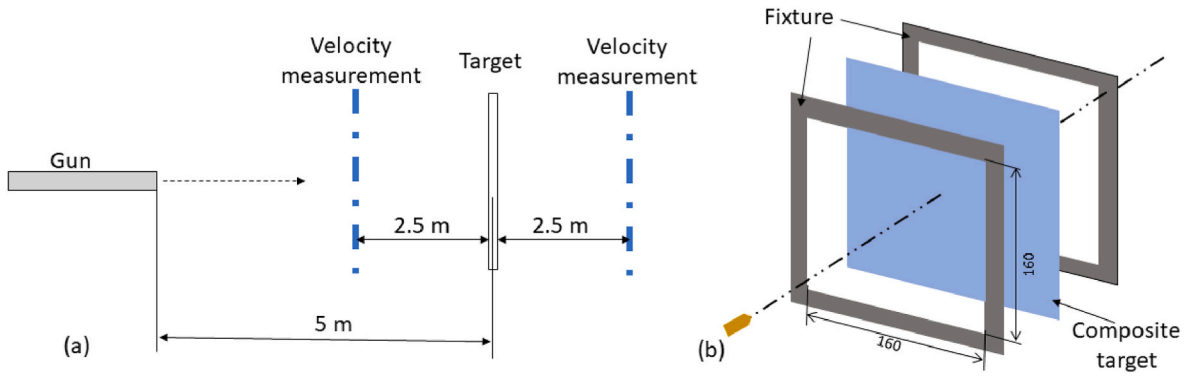

Fig. 4. Experimental setup for the ballistic tests of woven composites: (a) overall setup; (b) target and fixture.

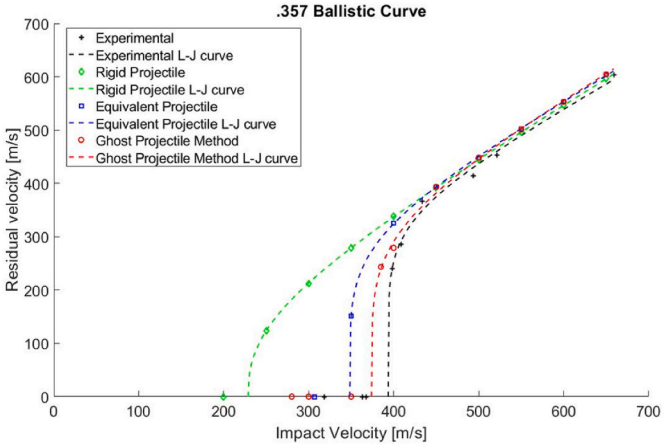

Fig. 5. Comparison among different analytical models (rigid projectile method from Ref. [32]; equivalent projectile method from Ref. [30]; and ghost projectile method from the current work) and experimental data.

impact velocities can be found. In this region, shear plugging failure can be the dominate mechanism under impact loading, and the features which can affect the residual velocity, presented as typical shear failure, are more easily captured by a numerical method. But the mechanical behavior is much more complicated within a lower impact velocity range. Close to the ballistic limit the impact energy, which is proportional to the square of the bullet velocity, is comparable with the maximum energy that can be absorbed by the target, therefore even slight differences in the modeling approaches may significantly vary the results. The results from the analytical model are closer to the experimental data than the ones from finite element method, especially on the threshold velocity for the penetration of the target. On the other hand, the energy absorption capability is another validation of the numerical models, as shown in Fig. 6b. The finite element model provides better correlation, when compared to the analytical model, with the penetrated targets, which may attribute to the element deletion feature in the finite element model. However, a large difference can be found for the non-penetrated cases, where the results from analytical models are more accurate. The same conclusions obtained by the analysis of the residual velocity curves can therefore be obtained based on energy absorption capacity. Considering there are many empirical input parameters in the material model used inside the finite element method for composite target (such as Coulomb's friction angle and coefficients for strain softening, which can be hardly determined by experiments), the accuracy of the results from the finite element method can vary from case to case, especially for composites with different types of constituents. Regarding the analytical model, most of the parameters involved can be obtained according to the physics of the materials, therefore presenting better performance on replication of the ballistic behavior of composites. Similar phenomena, i.e. the analytical model has more accurate predictions of the residual velocity compared with finite element method, can also be found in the series of existing works from Bresciani et al. [6,32]. But the consideration of other physical issues, such as yaw of projectile, may help to improve the results from finite element model [6].

Focusing on the projectile, its deformation from different numerical model with and without penetration of the target can be found in Fig. 7. More attention can be put on the angle obtained by deformation of the bullet tip, presented in the figure, which can be useful to describe the level of the deformation of the bullet. When the target stops the projectile (see Fig. 7a), a blunt tip is obtained from the analytical model,

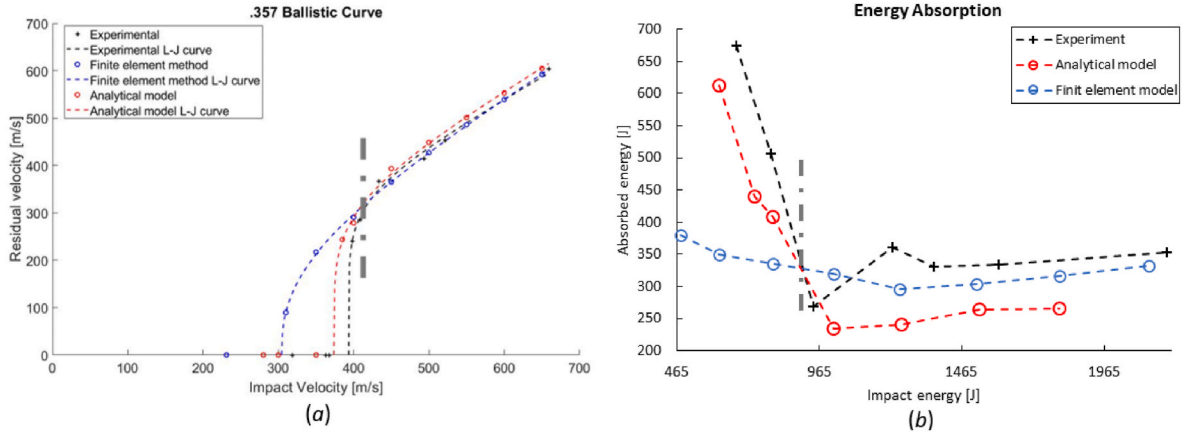

Fig. 6. Comparison of the numerical models and experimental data in the current work: (a) velocity; (b)energy absorption.

indicating a larger contact/damage region on the target, when compared with the finite element method. Thus, more energy is absorbed from the target, requiring higher energy/impact velocity for the penetration, which explains the difference of the ballistic limit between the analytical model and finite element method as shown in Fig. 6. As soon as penetration occurs (presented in Fig. 7b), the difference between the analytical model and finite element method on the deformation of the projectile is reduced, meaning comparable results from both numerical methods regarding energy dissipation.

The velocity history of the projectile from both the analytical model and finite element method with and without penetration of the target is presented in Fig. 8. Here, the normalized contact time was used, named as contact history in the figures, instead of the real contact time considering the different time scale between both models due to no friction effect in analytical model. For the non-penetrated case (impact velocity equal to 280 m/s in Fig. 8a), the reduction of the velocity from the analytical model is more significant than the one from the finite element method at the beginning, which can be recognized by the slope of the curves. While the opposite trend can be noticed on the analytical model after 10 % of the contact, where the changing on the slope indicates the main loading transfers from the jacket to the core of the projectile. Compared to the history from the analytical model, the curve from the finite element method is smoother because of the contact algorithm between the core and jacket in the model. The analytical model shows a larger energy absorbed by the target than finite element method due to the larger velocity reduction of the projectile while in contact with the target, corresponding to the conclusion about the larger deformation, i.e., larger contact area, in Fig. 7a. For the case with penetration of the target, the velocity history of the projectile from both numerical methods is comparable as presented in Fig. 8b. But the sharp corner on the curve can still be found at 45 % of the contact history from the analytical model, due to the different mechanical behavior of the jacket and core of the projectile during the impact. Moreover, the time for the loading passing from the jacket to the core is postponed by 10 % (non-penetration case) to 45 % (penetration case). This means that the jacket acts as a more important role for the penetration of the target than the core while the conclusion is opposite when the target stops the projectile. However, as also presented in the finite element method in Fig. 7, the core would be the final part contacting with the target, which causes more damage on the target due to its large extension along with the spalling of the jacket. On the other hand, the calculation time for each finite element model is around 45 min with 15 CPUs CPU (E5-2630v3 2.40 GHz 16 core/32 threads – 128 GB RAM), while it takes 2 min with one same CPU for each analytical model, presenting the efficiency of the latter one.

5. Conclusions

In the current work, both analytical model and finite element method have been used for ballistic simulation of the woven composite. Based on a review of the existing analytical models, an energy-based analytical model for ballistic simulation has been built; the lack of accuracy in the modeling of the full metal jacket projectile (with separate jacket and core) has been also pointed out. An innovative analytical model, named as ghost projectile method, was proposed based on an energy model, allowing the separate modeling of jacket and core of the projectile. As for the finite element method, an optimized MAT_162 was used in Ls-Dyna to assess the damage evolution of woven composites during impact. To validate the current model and study the capability of these numerical models, ballistic tests with woven Kevlar/epoxy as target and 0.357 Magnum (a full metal jacket soft core projectile) as the projectile were performed. The comparison of the numerical models and experimental data evaluated the accuracy of the proposed ghost projectile method, while the capability of both finite element method and analytical model has been investigated based on the ballistic curves, the loading history, and the deformation of the projectile.

The main conclusions are list as below.

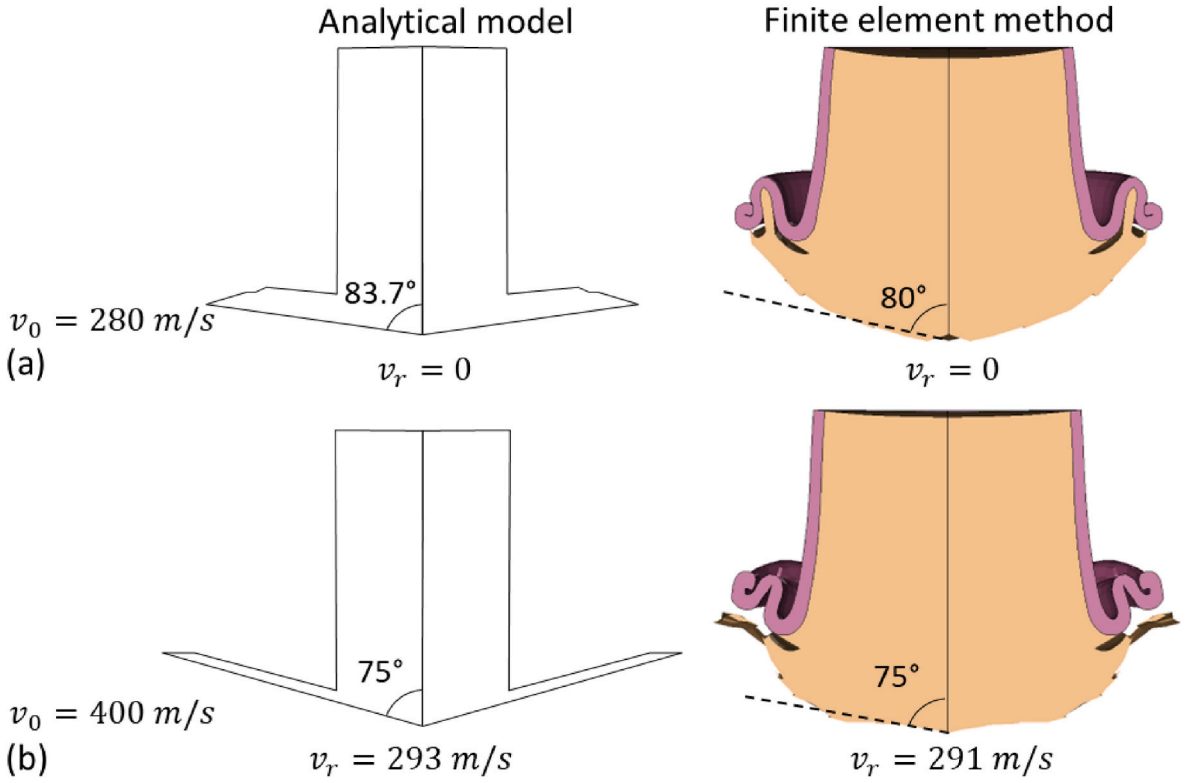

Fig. 7. Deformation of the projectile from the analytical model and finite element method with impact velocity of 280 m/s (a) and 400 m/s (b).

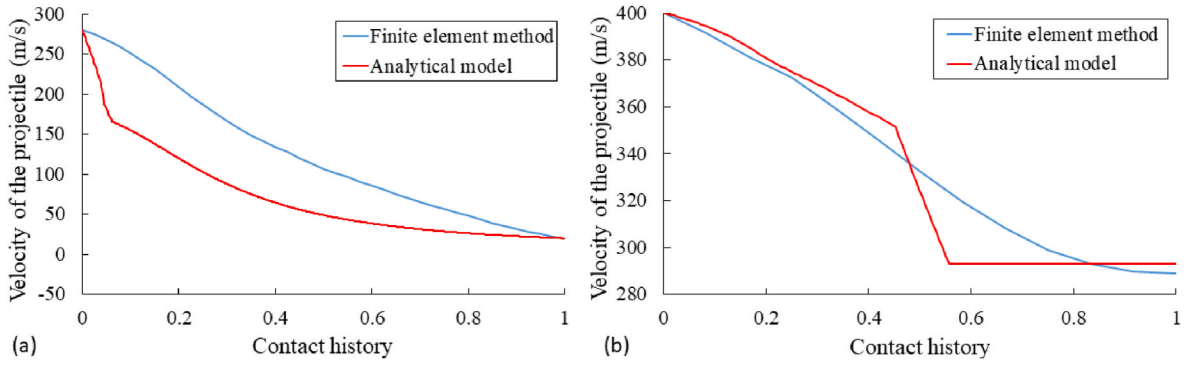

Fig. 8. Comparison of the velocity history of the projectile from the analytical model and finite element method: (a) $v_0 = 280m/s$; (b) $v_0 = \frac{400m}{s}$.

- The ghost projectile method allows to separately model the jacket and core of the projectile and can provide accurate predictions on the residual velocity.
- The analytical model (ghost projectile method) has better performance on the replication of the ballistic curve with higher efficiency compared to the finite element method under low impact velocities, especially at the ballistic limit.
- The deformation of the projectile can be replicated by the ghost projectile method, and it is comparable with the results from the finite element method (MAT_162) in the penetration cases of impact.
- The finite element method can provide more detailed deformation and damage phenomena for both target and projectile compared to the results from the analytical model.

CRediT authorship contribution statement

Dayou Ma: Conceptualization, Formal analysis, Investigation, Methodology, Software, Validation, Visualization, Writing – original draft. **Riccardo Scazzosi:** Investigation, Methodology, Validation, Writing – review & editing. **Andrea Manes:** Conceptualization, Resources, Visualization, Writing – review & editing.

Declaration of competing interest

The authors declare that they have no known competing financial interests or personal relationships that could have appeared to influence the work reported in this paper.

Data availability

Data will be made available on request.

References

[1] P.V. Cavallaro, Effects of weave Styles and Crimp Gradients in woven Kevlar/epoxy composites, Exp. Mech. 56 (2016) 617–635, https://doi.org/10.1007/s11340-015-0075-4.
[2] Z. Guoqi, W. Goldsmith, C.K.H. Dharan, Penetration of laminated Kevlar by projectiles-I. Experimental investigation, Int J Solids Struct 29 (1992) 399–420, https://doi.org/10.1016/0020-7683(92)90207-A.
[3] D. Zhang, Y. Sun, L. Chen, S. Zhang, N. Pan, Influence of fabric structure and thickness on the ballistic impact behavior of Ultrahigh molecular weight polyethylene composite laminate, Mater. Des. 54 (2014) 315–322, https://doi.org/10.1016/J.MATDES.2013.08.074.
[4] W. Wijaya, M.A. Ali, R. Umer, K.A. Khan, P.A. Kelly, S. Bickerton, An Automatic methodology to CT-scans of 2D woven Textile fabrics to structured finite element and Voxel Meshes, Compos Part A Appl Sci Manuf (2019) 105561, https://doi.org/10.1016/J.COMPOSITESA.2019.105561.
[5] D. Shoukroun, L. Massimi, F. Iacoviello, M. Endrizzi, D. Bate, A. Olivo, et al., Enhanced composite plate impact damage detection and characterisation using X-Ray refraction and scattering contrast combined with ultrasonic imaging, Compos Part B Eng (2019) 107579, https://doi.org/10.1016/J.COMPOSITESB.2019.107579.
[6] L.M. Bresciani, A. Manes, A. Ruggiero, G. Iannitti, M. Giglio, Experimental tests and numerical modelling of ballistic impacts against Kevlar 29 plain-woven fabrics with an epoxy matrix: Macro-homogeneous and Meso-heterogeneous approaches, Compos Part B Eng 88 (2016) 114–130, https://doi.org/10.1016/j.compositesb.2015.10.039.
[7] M.V. Zhikharev, S.B. Sapozhnikov, Two-scale modeling of high-velocity fragment GFRP penetration for assessment of ballistic limit, Int. J. Impact Eng. 101 (2017) 42–48, https://doi.org/10.1016/j.ijimpeng.2016.08.005.
[8] D. Ma, A. Manes, S.C. Amico, M. Giglio, Ballistic strain-rate-dependent material modelling of glass-fibre woven composite based on the prediction of a meso-heterogeneous approach, Compos. Struct. 216 (2019) 187–200, https://doi.org/10.1016/j.compstruct.2019.02.102.
[9] Z. Zhao, H. Dang, C. Zhang, G.J. Yun, Y. Li, A multi-scale modeling framework for impact damage simulation of triaxially braided composites, Compos Part A Appl Sci Manuf 110 (2018) 113–125, https://doi.org/10.1016/J.COMPOSITESA.2018.04.020.
[10] X. Li, D. Ma, H. Liu, W. Tan, X. Gong, C. Zhang, et al., Assessment of failure criteria and damage evolution methods for composite laminates under low-velocity impact, Compos. Struct. 207 (2019) 727–739, https://doi.org/10.1016/J.COMPSTRUCT.2018.09.093.
[11] J. Zhou, B. Liu, S. Wang, Finite element analysis on impact response and damage mechanism of composite laminates under single and repeated low-velocity impact, Aerosp Sci Technol 129 (2022) 107810, https://doi.org/10.1016/J.AST.2022.107810.
[12] R. Scazzosi, A. Manes, G. Petrone, M. Giglio, Two different modelling approaches for fabric composites subjected to ballistic impact, IOP Conf. Ser. Mater. Sci. Eng. 406 (2018), https://doi.org/10.1088/1757-899X/406/1/012051.
[13] A. Matzenmiller, J. Lubliner, R.L. Taylor, A constitutive model for anisotropic damage in fiber-composites, Mech. Mater. 20 (1995) 125–152, https://doi.org/10.1016/0167-6636(94)00053-0.
[14] E. Giannaros, A. Kotzakolios, G. Sotiriadis, S. Tsantzalis, V. Kostopoulos, On fabric materials response subjected to ballistic impact using meso-scale modeling. Numerical simulation and experimental validation, Compos. Struct. 204 (2018) 745–754, https://doi.org/10.1016/J.COMPSTRUCT.2018.07.090.
[15] D. Ginzburg, F. Pinto, O. Iervolino, M. Meo, Damage tolerance of bio-inspired helicoidal composites under low velocity impact, Compos. Struct. 161 (2017) 187–203, https://doi.org/10.1016/J.COMPSTRUCT.2016.10.097.
[16] R. Scazzosi, M. Giglio, A. Manes, Numerical simulation of high-velocity impact on fiber-reinforced composites using MAT_162, Mater Des Process Commun 3 (2021) e163, https://doi.org/10.1002/MDP2.163.
[17] L. Maio, E. Monaco, F. Ricci, L. Lecce, Simulation of low velocity impact on composite laminates with progressive failure analysis, Compos. Struct. 103 (2013) 75–85, https://doi.org/10.1016/j.compstruct.2013.02.027.
[18] D. Ma, Á. González-Jiménez, M. Giglio, C.M. dos Santos Cougo, S.C. Amico, A. Manes, Multiscale modelling approach for simulating low velocity impact tests of aramid-epoxy composite with nanofillers, Eur J Mech - A/Solids (2021) 104286, https://doi.org/10.1016/j.euromechsol.2021.104286.
[19] R. Scazzosi, A. Manes, M. Giglio, An Enhanced material model for the simulation of high-velocity impact on fiber-reinforced composites, Procedia Struct. Integr. 24 (2019) 53–65, https://doi.org/10.1016/j.prostr.2020.02.005.
[20] B. Gu, Analytical modeling for the ballistic perforation of planar plain-woven fabric target by projectile, Compos Part B Eng 34 (2003) 361–371, https://doi.org/10.1016/S1359-8368(02)00137-3.
[21] G. Caprino, Influence of material thickness on the response of carbon-fabric/epoxy panels to low velocity impact, Compos. Sci. Technol. 59 (1999) 2279–2286, https://doi.org/10.1016/S0266-3538(99)00079-2.
[22] Z. Zhu, X. Li, R. Yang, Z. Ye, Q. Teng, A modified model to predict the ballistic limit of a cubic fragment penetrating Kevlar/titanium fiber metal laminate, Int. J. Impact Eng. 168 (2022) 104292, https://doi.org/10.1016/j.ijimpeng.2022.104292.
[23] L. Jintao, L. Moubin, An analytical model to predict the impact of a bullet on ultra-high molecular weight polyethylene composite laminates, Compos. Struct. 282 (2022) 115064, https://doi.org/10.1016/j.compstruct.2021.115064.
[24] G. Caprino, A. Langella, V. Lopresto, Prediction of the first failure energy of circular carbon fibre reinforced plastic plates loaded at the centre, Compos Part A Appl Sci Manuf 34 (2003) 349–357, https://doi.org/10.1016/S1359-835X(03)00026-5.

[25] N.K. Naik, P. Shrirao, Composite structures under ballistic impact, Compos. Struct. 66 (2004) 579–590, https://doi.org/10.1016/j.compstruct.2004.05.006.
[26] M. Mamivand, G.H. Liaghat, A model for ballistic impact on multi-layer fabric targets, Int. J. Impact Eng. 37 (2010) 806–812, https://doi.org/10.1016/j.ijimpeng.2010.01.003.
[27] L. Peng, M.T. Tan, X. Zhang, G. Han, W. Xiong, M. Al Teneiji, et al., Investigations of the ballistic response of hybrid composite laminated structures, Compos. Struct. 282 (2022) 115019, https://doi.org/10.1016/j.compstruct.2021.115019.
[28] D. Gregori, R. Scazzosi, S.G. Nunes, S.C. Amico, M. Giglio, A. Manes, Analytical and numerical modelling of high-velocity impact on multilayer alumina/aramid fiber composite ballistic shields: improvement in modelling approaches, Compos Part B Eng 187 (2020) 107830, https://doi.org/10.1016/j.compositesb.2020.107830.
[29] T. Børvik, S. Dey, A.H. Clausen, Perforation resistance of five different high-strength steel plates subjected to small-arms projectiles, Int. J. Impact Eng. 36 (2009) 948–964, https://doi.org/10.1016/J.IJIMPENG.2008.12.003.
[30] R. Scazzosi, A. Manes, M. Giglio, Analytical model of high-velocity impact of a deformable projectile against Textile-based composites, J. Mater. Eng. Perform. 28 (2019) 3247–3255, https://doi.org/10.1007/S11665-019-04026-X/TABLES/3.
[31] N.K. Naik, P. Shrirao, B.C.K. Reddy, Ballistic impact behaviour of woven fabric composites: formulation, Int. J. Impact Eng. 32 (2006) 1521–1552, https://doi.org/10.1016/J.IJIMPENG.2005.01.004.
[32] L.M. Bresciani, A. Manes, M. Giglio, An analytical model for ballistic impacts against plain-woven fabrics with a polymeric matrix, Int. J. Impact Eng. 78 (2015) 138–149, https://doi.org/10.1016/j.ijimpeng.2015.01.001.
[33] Z. Guoqi, W. Goldsmith, C.K.H. Dharan, Penetration of laminated Kevlar by projectiles—I. Experimental investigation, Int J Solids Struct 29 (1992) 399–420, https://doi.org/10.1016/0020-7683(92)90207-A.
[34] S. Morye, P. Hine, R. Duckett, D. Carr, I. Ward, Modelling of the energy absorption by polymer composites upon ballistic impact, Compos. Sci. Technol. 60 (2000) 2631–2642, https://doi.org/10.1016/S0266-3538(00)00139-1.
[35] R.F. Recht, T.W. Ipson, Ballistic perforation Dynamics, J. Appl. Mech. 30 (1963) 384–390, https://doi.org/10.1115/1.3636566.
[36] M. Rezasefat, A. Gonzalez-Jimenez, M. Giglio, A. Manes, An evaluation of Cuntze and Puck inter fibre failure criteria in simulation of thin CFRP plates subjected to low velocity impact, Compos. Struct. 278 (2021) 114654, https://doi.org/10.1016/J.COMPSTRUCT.2021.114654.
[37] Naik NK, Kumar S, Ratnaveer D, Joshi M, Akella K. An Energy-Based Model for Ballistic Impact Analysis of Ceramic-Composite Armors: Https://DoiOrg/101177/1056789511435346 2012;22:145–87.https://doi.org/10.1177/1056789511435346..
[38] E. Cen, 1522—Windows, Doors, Shutters and Blinds-Bullet Resistance—Requirements and Classification, 1998.
[39] LS-DYNA Keyword User's Manual, 2018.
[40] J.R. Xiao, B.A. Gama, J.W. Gillespie, Progressive damage and delamination in plain weave S-2 glass/SC-15 composites under quasi-static punch-shear loading, Compos. Struct. 78 (2007) 182–196, https://doi.org/10.1016/J.COMPSTRUCT.2005.09.001.
[41] D. Ma, Z. Wang, M. Giglio, S. Campos Amico, A. Manes, Influence of strain-rate related parameters on the simulation of ballistic impact in woven composites, Compos. Struct. (2022) 116142, https://doi.org/10.1016/J.COMPSTRUCT.2022.116142.
[42] G.R. Johnson, W.H. Cook, Fracture characteristics of three metals subjected to various strains, strain rates, temperatures and pressures, Eng. Fract. Mech. 21 (1985) 31–48, https://doi.org/10.1016/0013-7944(85)90052-9.
[43] Lambert JP, Jonas GH. Towards Standardization in Terminal Ballistics Testing: Velocity Representation 1976. https://doi.org/10.21236/ADA021389..